Iğdır Üniversitesi Fen Bilimleri Enstitüsü Dergisi, 15(2), 615-623, 2025
Journal of the Institute of Science and Technology, 15(2), 615-623, 2025

ISSN: 2146-0574, eISSN: 2536-4618

Kimya / *Chemistry* **DOI: 10.21597/jist.1545430**

Araştırma Makalesi / *Research Article*

Geliş tarihi / *Received*: 08.09.2024 **Kabul tarihi / *Accepted*: 25.10.2024**

Atıf İçin: Öztürk Doğan, H. ve Sezgin, M. (2025). Grafen Oksit Miktarının In_2O_3-İndirgenmiş Grafen Oksit Kompozit Filminin Yapısı ve Morfolojisi Üzerindeki Etkisi. *Iğdır Üniversitesi Fen Bilimleri Enstitüsü Dergisi*, 15(2), 615-623.

To Cite: Öztürk Doğan, H. & Sezgin, M. (2025). Influence of Graphene Oxide Amount on The Structure And Morphology of In_2O_3-Reduced Graphene Oxide Composite Film. Journal of the Institute of Science and Technology, 15(2), 615-623.

Grafen Oksit Miktarının In_2O_3-İndirgenmiş Grafen Oksit Kompozit Filminin Yapısı ve Morfolojisi Üzerindeki Etkisi

Hülya ÖZTÜRK DOĞAN[1*], Mertcan SEZGİN[2]

Öne Çıkanlar:
- In_2O_3-rGO nanokompozitleri elektrokimyasal teknik kullanılarak üretildi.
- Nanokompozit yapısı ve morfolojisi üzerine GO miktarının etkisi araştırıldı.
- Değişen GO miktarları için In_2O_3-rGO nanokompozitleri üretildi.
- En optimum hacim oranı 1In:1GO olarak tespit edildi.

ÖZET:

Bu çalışmada, elektrokimyasal bir teknik kullanılarak ilk defa tek kapta indiyum oksitle indirgenmiş grafen oksit (In_2O_3-rGO) kompozitleri üretildi. Grafen oksit (GO) miktarının kompozit yapının kompozisyonu ve morfolojisi üzerindeki etkisi incelendi. Bu amaçla, GO ve In^{3+} iyonları içeren elektrolit çözeltileri farklı hacim oranlarında karıştırıldı. Biriktirmeler farklı elektrolit kompozisyonlarında sabit potansiyelde gerçekleştirildi. Farklı deneysel parametreler altında hazırlanan kompozit yapıların karakterizasyonları X-ışını kırınım spektroskopisi (XRD), X-ışını fotoelektron spektroskopisi (XPS), Raman spektroskopisi ve alan etkili taramalı elektron mikroskobu (FESEM) teknikleri kullanılarak incelendi. En iyi kompozisyona sahip In_2O_3-rGO kompozitinin hacimce 1:1 GO:In^{3+} elektrolit oranında elde edildiği sonucuna varıldı.

Anahtar Kelimeler:
- Elektrokimyasal depozisyon
- İndiyum oksit
- Nanokompozit
- İndirgenmiş grafen oksit

Influence Of Graphene Oxide Amount on The Structure and Morphology of In_2O_3-Reduced Graphene Oxide Composite Film

Highlights:
- In_2O_3-rGO nanocomposites were produced using electrochemical technique.
- The effect of GO amount on nanocomposite structure and morphology was investigated.
- In_2O_3-rGO nanocomposites were produced for varying GO amounts.
- The most optimum volume ratio was determined as 1In:1GO.

ABSTRACT:

In this study, indium oxide-reduced graphene oxide (In_2O_3-rGO) composites were produced in one-pot using an electrochemical technique for the first time. The effect of graphene oxide (GO) amount on the composition and morphology of the composite structure was investigated. For this purpose, electrolyte solutions containing GO and In^{3+} ions were mixed at different volume ratios. Deposits were carried out at constant potential in different electrolyte compositions. The characterizations of the composite structures prepared under different experimental parameters were investigated using X-ray diffraction spectroscopy (XRD), X-ray photoelectron spectroscopy (XPS), Raman spectroscopy, and field effect scanning electron microscopy (FESEM) techniques. It was concluded that the In_2O_3-rGO composite with the best composition was obtained in 1:1 GO: In^{3+} electrolyte by volume.

Keywords:
- Electrochemical deposition
- Indium oxide
- Nanocomposite
- Reduced graphene oxide

[1] Hülya ÖZTÜRK DOĞAN (**Orcid ID:** 0000-0002-4072-7744), Atatürk University, Vocational School of Technical Sciences, Department of Chemistry and Chemical Processing Technologies, Erzurum, Türkiye

[2]Mertcan SEZGİN (**Orcid ID:** 0009-0004-0504-8756), Atatürk University, Department of Nanoscience and Nanoengineering, Erzurum, Türkiye

***Sorumlu Yazar/*Corresponding Author*:** Hülya ÖZTÜRK DOĞAN, e-mail: hdogan@atauni.edu.tr

INTRODUCTION

Nanocrystalline metal oxides have many applications in magnetic data storage, batteries, catalysts, and sensors. Among various metal oxides, indium oxide (In_2O_3) is a remarkable n-type semiconductor metal oxide with a wide band gap (3.55–3.75 eV) (Prakash et al., 2011; L. Zhu et al., 2024). In_2O_3 nanostructures have been reported to exist in different morphologies, such as nanowires, nanorods, nanoparticles, nanospheres, nanosheets, microspheres, and microtubes (Zhu et al., 2007; Fang et al., 2022). In_2O_3 nanocrystals are widely used in many potential applications, such as microelectronic device materials in solar cells, transparent conductors, gas sensors, touch panel displays, photocatalysis, sensors, lithium-ion batteries, and light-emitting diodes (Anand et al., 2016; Sekkat et al., 2024).

In_2O_3 offers advantages such as the location of the conduction and valence band edges, which have excellent conductivity and stability for direct photoelectrolysis of water and the correct support of water redox potentials. However, In_2O_3's large band gap exhibits low conversion efficiency when utilizing visible light. Adding dopants to the In_2O_3 lattice can improve optical and electrical properties. Researchers have shown that doping In_2O_3 with metal cations such as Nb, Al, Sn, W, Ti, V, and Mo significantly affects optoelectronic properties (Mostafa et al., 2018). In addition, carbon-based materials such as graphene, graphene oxide (GO), and reduced graphene oxide (rGO) can also be preferred for this purpose (Doğan, 2019; Doğan et al., 2019; Eryiğit et al., 2022). rGO, the rising star of the carbon family, has a thick planar layer consisting of a sp^2-bonded carbon structure. Like graphene, rGO is a type of material with some extraordinary properties, such as ultra-large specific surface area, flexibility, high electrical conductivity, superior chemical stability, and exceptional mechanical strength. The rGO structure can be easily obtained by reducing GO using various techniques such as chemical, electrochemical, and hydrothermal. The literature describes different techniques for the synthesis of In_2O_3-graphene composites, such as supercritical fluid (Ioni et al., 2021), hydrothermal synthesis (Mao et al., 2024), microwave-assisted synthesis (Alaizeri et al., 2023), and etc. However, one-pot electrochemical synthesis of In_2O_3-graphene nanostructures has not been performed so far. Nitrate ions have an important role in the nanocomposite formation mechanism between In_2O_3 and rGO during electrodeposition (Kurt Urhan et al., 2019). The reduction of GO to rGO simultaneously occurs through the formation of hydroxide and the conversion to the metal oxide form.

In general, spin coating, hydrothermal synthesis, spray pyrolysis, electrodeposition, microwave-assisted synthesis, and inkjet printing coatings are among the most widely used techniques for the synthesis of metal oxide thin films (Mostafa et al., 2018). Most of these methods are performed with toxic organic solvents and surfactants (Vakh & Koronkiewicz, 2023; Younis & Osman, 2023). Moreover, the reaction parameters include high temperature and long reaction times. The electrodeposition technique has many advantages, such as direct production on the electrode surface, low cost, and easy application.

In this study, In_2O_3-rGO nanocomposites were synthesized by the one-pot electrochemical deposition method. In_2O_3-rGO nanocomposites with different GO amounts were prepared, and structural and morphological characterizations of all samples were performed. Among these samples, the nanocomposite structure in the GO:In^{3+} electrolyte mixture with a volume ratio 1:1 was found to have the best morphology and composition.

MATERIALS AND METHODS

Synthesis of In_2O_3-rGO

10mM indium chloride ($InCl_3$) salt was used as the source of In^{3+} ions. Graphene oxide (GO), $InCl_3$, and potassium nitrate (KNO_3) were supplied by Sigma. To prepare the GO suspension, 1mL containing 2mg/mL GO (2mg GO/1mL H_2O) was added to 0.1 M 10mL KNO_3 solution. GO and In^{3+} solutions were mixed in varying volumetric ratios such as 1:1, 2:1, and 1:2. BASi100 model potentiostat was used for the electrochemical deposition of In_2O_3-rGO nanocomposites. The working, counter, and reference electrodes in the three-electrode cell system were indium tin oxide coated glass (ITO), Pt wire, and Ag/AgCl electrodes. The deposition potential of In_2O_3-rGO nanocomposites was determined as −1.4 V by recording a cyclic voltammogram (CV).

Characterization of In_2O_3-rGO

For the structural characterization of the produced In_2O_3-rGO nanocomposites, x-ray diffraction spectroscopy (XRD, Rigaku MiniFlex Benchtop Powder XRD Diffractometer 2005E302 model), x-ray photoelectron spectroscopy (XPS, Specs-Flex trademark) and Raman spectroscopy (WITech alpha 300R) techniques were used. Morphological characterization was performed using field emission scanning electron microscopy (FE-SEM, Zeiss Sigma 300). XRD analyses were recorded using Cu Kα radiation (λ = 1.5405 Å) at 2tetha between 10 and 80 degrees with 4-degree steps. Core-level XPS analyses were measured with a sensitivity of 0.1 eV. Raman spectrum was analyzed using a 532 nm and 100mW laser source.

RESULTS AND DISCUSSION

Structural Analysis

To determine the phase structure of In_2O_3-rGO nanocomposite, XRD patterns of materials deposited in various volume ratios were collected in Figure 1a. All XRD spectra presented in Fig. 1a show well-defined peaks at 2θ = 21.53°, 30.65°, 51.07°, 60.70° corresponding to (211), (222), (440) and (622) planes of In_2O_3 (Shifu et al., 2010, JCPDS card No. 89-4595). In addition, diffraction peaks related to the graphite crystal structure originating from rGO are also present. Besides, no diffraction peaks belonging to impurity species such as metallic In or $In(OH)_3$ are obtained in the XRD spectrum of the nanocomposite.

To examine different C types, number of graphene layers, and structural defects of In_2O_3-rGO nanocomposite, Raman spectroscopy was recorded as shown in Fig. 1b. In the 2In:1GO nanocomposite as volume ratio, the Raman spectrum of In_2O_3 film appeared as a plateau curve. When the volume ratio was changed to 1In:1GO, a spectrum with some peaks related to the vibration modes E_{1g} (131 and 304 1/cm), E_{2g} (626 1/cm), A_{1g} (494 1/cm) and 364 1/cm associated with In_2O_3 was obtained in the Raman spectrum (Gan et al., 2013; Wiranwetchayan et al., 2018). In addition, D (1330 1/cm) and G (1560 1/cm) bands originating from rGO were also observed. However, only the peaks belonging to rGO were present when the volume ratio was 1In:2GO. As a result, both In_2O_3 and rGO peaks in the deposited films occurred in the 1In:1GO mixture.

XPS analysis was performed to determine the chemical composition and bonding state of the elements in the nanocomposite film. Figure 2a shows the XPS spectrum of In 3d core levels. The binding energy of In 3d detected at 443.9 eV corresponds to In 3d5/2. The peak corresponding to In 3d3/2 was detected at 451.5 eV. The difference between the In 3d3/2 and In 3d5/2 peaks is 7.6 eV, confirming the presence of In^{3+} in In_2O_3 nanoparticles (Sawant et al., 2021). Moreover, the XPS spectrum of In3d for In_2O_3 has broader spectral components than metallic In. For these reasons, it can

be said that the In_2O_3-rGO nanocomposite contains the In_2O_3 structure. Figure 2b shows the XPS O 1s core level spectra of the nanocomposites prepared at different concentration ratios. It is generally known that the oxygen 1s core levels of crystalline metal oxides are located in the relatively narrow binding energy range of 529.0 eV–531.1 eV (Zatsepin et al., 2019). The 530.3 eV band belongs to the XPS O 1s core level signal coming from the regular oxygen sublattice of In_2O_3 (Gurlo et al., 1997). In addition, the peak in the 529.0 eV region allows us to conclude that adsorbed OH groups or GO is due to the presence of entirely non-reducing oxygen groups.

To determine the reduction of GO to rGO, C1s core level XPS spectrum was recorded (Figure 2c). C1s spectrum for GO contains two main peak regions: C-C/C=C at 284 eV-286 eV and C-O functional groups at 286 eV-289 eV (Al-Gaashani et al., 2019; Öztürk Doğan & Kurt Urhan, 2023). In the spectrum in Figure 2c, as the GO ratio increases in In_2O_3-rGO nanocomposite, the peak in the 287 eV region was obtained more dominantly. Oxygen functional group peaks also decrease depending on the decrease of GO amount in the In:GO ratio. Similarly, increasing the GO amount also increased the peak intensity of the C-C bond. For In_2O_3-rGO nanocomposites prepared at varying concentration ratios, it was determined that the most suitable composition for the reduction degrees of GO was a 1In:1GO ratio. When the In3d, O1s, and C1s XPS spectra of the nanocomposites prepared at varying concentration ratios were examined, the 1In:1GO ratio was chosen due to the presence of In^{3+} in the In3d peak, the lattice O1s peak, and the absence of oxygenated functional groups of GO. Furthermore, the atomic percentage values of each element were investigated using the data in the general scanning XPS spectra. Table 1 shows the changes in the ratio of the In, O, and C elements in the In_2O_3-rGO nanostructures produced at different concentration ratios. As seen in Table 1, different concentrations also affected the element distribution within the nanostructure. It was supported that the most suitable composition for the In:O:C composition ratio was 1In:1GO.

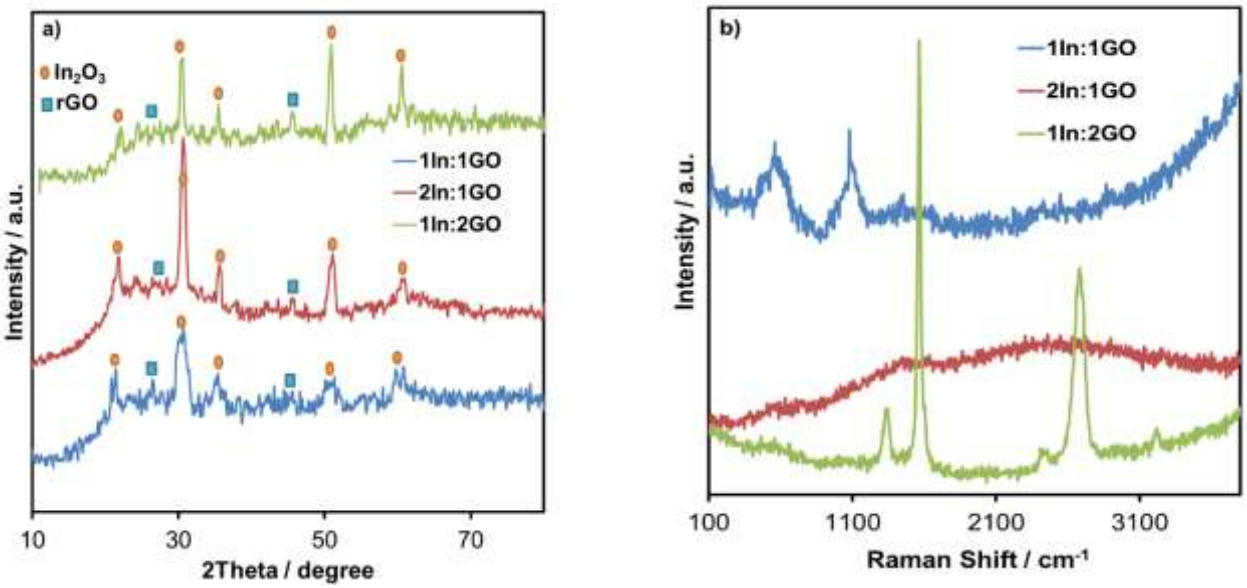

Fig. 1. XRD **(a)** and Raman **(b)** spectrum of In_2O_3-rGO nanocomposite

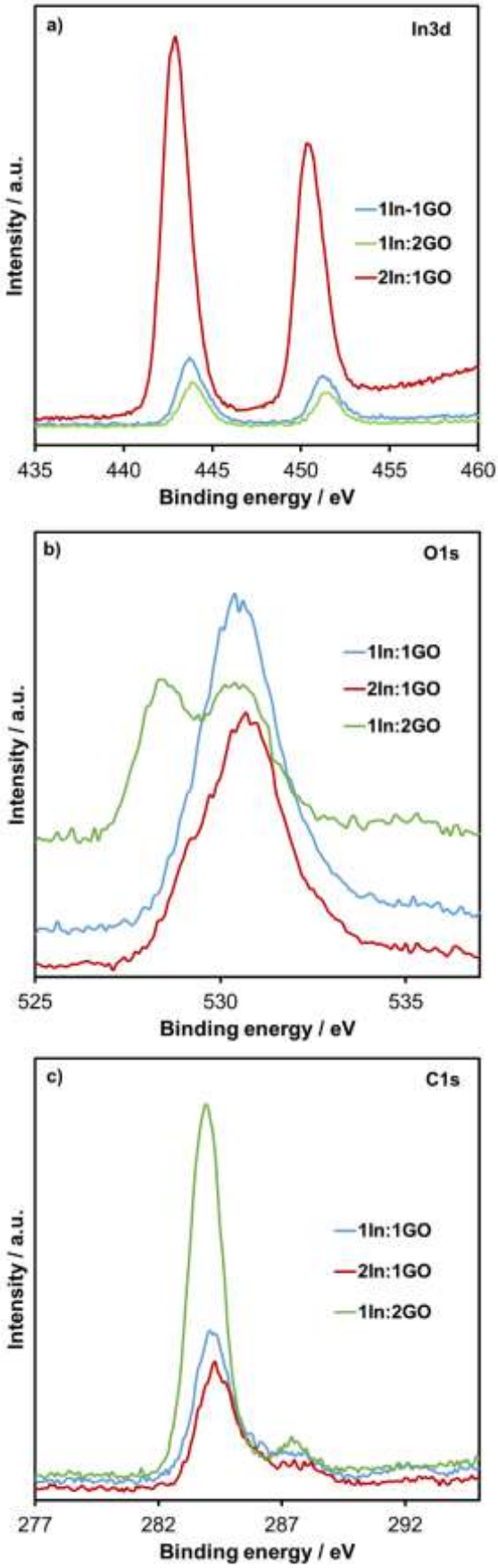

Fig. 2. High-resolution XPS of In 3d (a), O 1s (b), C 1s (c) core-levels for In_2O_3-rGO nanocomposite

Table 1. Changes of the In, O, and C elements in the In_2O_3-rGO nanostructures produced at different concentration ratios

Volume ratio of In:GO	In	O	C
1:2	12.35	26.59	61.06
2:1	36.6	38.27	25.13
1:1	23.25	49.47	27.28

Morphological Analysis

The surface morphology of the prepared In_2O_3-rGO nanocomposites was investigated using FESEM. Figure 3 shows the FESEM images of the nanocomposites produced with varying amounts of GO. In Figure 3a, it is seen that bulk graphene structures are formed on the surface due to the increasing amount of GO for the FESEM image of the 1In:2GO sample at x10000 magnification. In addition, the presence of In_2O_3 structures is also evident in the lower layer of these rGO layers for x40000 magnification. As shown in Figure 3b, spherical In_2O_3 structures distributed uniformly on the surface were obtained due to the increase in the amount of In (for 2In:1GO). This may be due to the faster kinetics of In^{3+} ions accumulating on the electrode surface during electrochemical deposition compared to rGO. In the FESEM image given in Figure 3c, it is clearly seen that the In_2O_3-rGO nanocomposite for the 1In:1GO ratio contains both nanoparticles and graphene sheets with suitable morphology.

EDX spectra recorded for all samples (Figure 3) show that In, O, and C elements are present in the chemical composition of In_2O_3-rGO nanostructures without any impurity elements. Moreover, the elemental compositions showed variations that confirmed the ratios in the composite. When the amount of GO increased, the percentage of C increased; when the amount of In increased, the percentage of In increased. FESEM images and EDS analysis are in good agreement with previous results (Table 2). All results show that In_2O_3-rGO nanostructures were successfully prepared using an electrochemical technique.

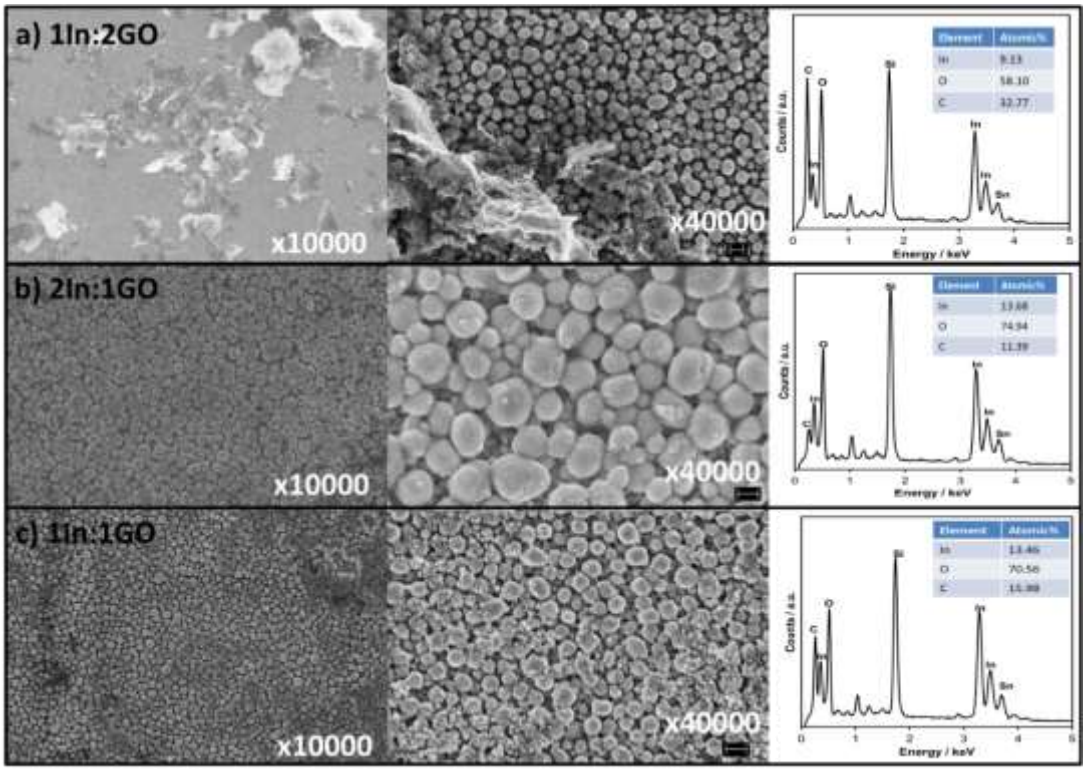

Fig. 3. FESEM images and EDS spectra of In_2O_3-rGO nanocomposite for volume ratios of 1In:2GO (a), 2In:1GO (b), 1In:1GO (c)

Table 2. Morphology of In_2O_3 nanostructures depending on the production technique

Material	Technique	Morphology	Reference
In_2O_3	Chemical vapor deposition	Nanowire	(Tuzluca et al., 2018)
N-doped rGO–In_2O_3	Hydrothermal	Nanocube	(Shanmugasundaram et al., 2017)
In_2O_3–functionalized rGO	Chemical	Nanorods	(Guo et al., 2023)
In_2O_3	Ultrasonic-assisted synthesis	Nanoparticle	(El-Khouly et al., 2020)
In_2O_3/RGO	Microwave-assisted hydrothermal synthesis	Nanoparticle	(Alaizeri et al., 2023)
In_2O_3-rGO	Electrodeposition	Nanoparticle	This study

CONCLUSION

This study presents the effect of changing the amount of GO on the composition and morphology of the nanocomposite for electrochemical production of In_2O_3-rGO nanocomposites. For this purpose, In:GO concentration ratios were tested as 1:1, 1:2, and 2:1. It was determined that the optimum nanocomposite composition and morphology could be produced at the 1In:1GO ratio. XRD, Raman and XPS characterizations supported the fact that the composite composition was composed of In_2O_3 and rGO. As a result, it was seen that In_2O_3-rGO nanocomposites with the best composition could be synthesized using an electrochemical technique when the In:GO concentration ratio was 1:1.

Conflict of Interest

The article authors declare that there is no conflict of interest between them.

Author's Contributions

The authors declare that they have contributed equally to the article.

REFERENCES

Alaizeri, Z. M., Alhadlaq, H. A., Aldawood, S., Akhtar, M. J., Aziz, A. A., & Ahamed, M. (2023). Photocatalytic Degradation of Methylene Blue and Anticancer Response of In2O3/RGO Nanocomposites Prepared by a Microwave-Assisted Hydrothermal Synthesis Process. *Molecules*, *28*(13), Article 13. https://doi.org/10.3390/molecules28135153

Al-Gaashani, R., Najjar, A., Zakaria, Y., Mansour, S., & Atieh, M. A. (2019). XPS and structural studies of high quality graphene oxide and reduced graphene oxide prepared by different chemical oxidation methods. *Ceramics International*, *45*(11), 14439–14448. https://doi.org/10.1016/j.ceramint.2019.04.165

Anand, K., Kaur, J., Singh, R. C., & Thangaraj, R. (2016). Structural, optical and gas sensing properties of pure and Mn-doped In2O3 nanoparticles. *Ceramics International*, *42*(9), 10957–10966. https://doi.org/10.1016/j.ceramint.2016.03.233

Doğan, H. Ö. (2019). Ethanol electro-oxidation in alkaline media on Pd/electrodeposited reduced graphene oxide nanocomposite modified nickel foam electrode. *Solid State Sciences*, *98*, 106029. https://doi.org/10.1016/j.solidstatesciences.2019.106029

Doğan, H. Ö., Çepni, E., Urhan, B. K., & Eryiğit, M. (2019). Non-Enzymatic Amperometric Detection of H2O2 on One-Step Electrochemical Fabricated Cu2O/Electrochemically Reduced Graphene Oxide Nanocomposite. *ChemistrySelect*, *4*(28), 8317–8321. https://doi.org/10.1002/slct.201901588

El-Khouly, S. M., Fathy, N. A., Farag, H. K., & Aboelenin, R. M. M. (2020). In2O3 catalyst supported on carbonaceous nanohybrid for enhancing the removal of methyl orange dye from aqueous solutions. *Desalination and Water Treatment*, *174*, 344–353. https://doi.org/10.5004/dwt.2020.24840

Eryiğit, M., Kurt Urhan, B., Doğan, H. Ö., Özer, T. Ö., & Demir, Ü. (2022). ZnO Nanosheets-Decorated ERGO Layers: An Efficient Electrochemical Sensor for Non-Enzymatic Uric Acid Detection. *IEEE Sensors Journal*, *22*(6), 5555–5561. IEEE Sensors Journal. https://doi.org/10.1109/JSEN.2022.3150088

Fang, J., Ma, Z.-H., Xue, J.-J., Chen, X., Xiao, R.-P., & Song, J.-M. (2022). Au doped In2O3 nanoparticles: Preparation, and their ethanol detection with high performance. *Materials Science in Semiconductor Processing*, *146*, 106701. https://doi.org/10.1016/j.mssp.2022.106701

Gan, J., Lu, X., Wu, J., Xie, S., Zhai, T., Yu, M., Zhang, Z., Mao, Y., Wang, S. C. I., Shen, Y., & Tong, Y. (2013). Oxygen vacancies promoting photoelectrochemical performance of In2O3 nanocubes. *Scientific Reports*, *3*(1), 1021. https://doi.org/10.1038/srep01021

Guo, L., Liang, H., Hu, H., Shi, S., Wang, C., Lv, S., Yang, H., Li, H., de Rooij, N. F., Lee, Y.-K., French, P. J., Wang, Y., & Zhou, G. (2023). Large-Area and Visible-Light-Driven Heterojunctions of In2O3/Graphene Built for ppb-Level Formaldehyde Detection at Room Temperature. *ACS Applied Materials & Interfaces*, *15*(14), 18205–18216. https://doi.org/10.1021/acsami.3c00218

Gurlo, A., Ivanovskaya, M., Pfau, A., Weimar, U., & Göpel, W. (1997). Sol-gel prepared In2O3 thin films. *Thin Solid Films*, *307*(1), 288–293. https://doi.org/10.1016/S0040-6090(97)00295-2

Ioni, Y. V., Kraevsky, S. V., Groshkova, Y. A., & Buslaeva, E. Yu. (2021). Immobilization of In2O3 nanoparticles on the surface of reduced graphene oxide. *Mendeleev Communications*, *31*(5), 718–720. https://doi.org/10.1016/j.mencom.2021.09.042

Kurt Urhan, B., Öznülüer, T., Demir, Ü., & Öztürk Doğan, H. (2019). One-Pot Electrochemical Synthesis of Lead Oxide- Electrochemically Reduced Graphene Oxide Nanostructures and Their Electrocatalytic Applications. *IEEE Sensors Journal*, *19*(13), 4781–4788. IEEE Sensors Journal. https://doi.org/10.1109/JSEN.2019.2904738

Mao, Y., Jiang, Y., Liu, H., Jiang, Y., Li, M., Su, W., & He, R. (2024). Ambient electrocatalytic synthesis of urea by co-reduction of NO3− and CO2 over graphene-supported In2O3. *Chinese Chemical Letters*, *35*(3), 108540. https://doi.org/10.1016/j.cclet.2023.108540

Mostafa, N. Y., Badawi, A., & Ahmed, S. I. (2018). Influence of Cu and Ag doping on structure and optical properties of In2O3 thin film prepared by spray pyrolysis. *Results in Physics*, *10*, 126–131. https://doi.org/10.1016/j.rinp.2018.05.030

Öztürk Doğan, H., & Kurt Urhan, B. (2023). NiS@CuBi2O4/ERGO heterostructured electro-catalyst for enhanced hydrogen evolution reaction. *Micro and Nanostructures*, *183*, 207666. https://doi.org/10.1016/j.micrna.2023.207666

Prakash, R., Kumar, S., Ahmed, F., Lee, C. G., & Song, J. I. (2011). Room temperature ferromagnetism in Ni doped In2O3 nanoparticles. *Thin Solid Films*, *519*(23), 8243–8246. https://doi.org/10.1016/j.tsf.2011.03.105

Sawant, J. P., Pathan, H. M., & Kale, R. B. (2021). Spray Pyrolytic Deposition of CuInS2 Thin Films: Properties and Applications. *Engineered Science*, *Volume 13 (March 2021)*(8), 51–64.

Sekkat, A., Sanchez-Velasquez, C., Bardet, L., Weber, M., Jiménez, C., Bellet, D., Muñoz-Rojas, D., & Huong Nguyen, V. (2024). Towards enhanced transparent conductive nanocomposites based on metallic nanowire networks coated with metal oxides: A brief review. *Journal of Materials Chemistry A*, *12*(38), 25600–25621. https://doi.org/10.1039/D4TA05370B

Shanmugasundaram, A., Gundimeda, V., Hou, T., & Lee, D. W. (2017). Realizing Synergy between In2O3 Nanocubes and Nitrogen-Doped Reduced Graphene Oxide: An Excellent Nanocomposite for the Selective and Sensitive Detection of CO at Ambient Temperatures. *ACS Applied Materials & Interfaces*, *9*(37), 31728–31740. https://doi.org/10.1021/acsami.7b06253

Shifu, C., Xiaoling, Y., Huaye, Z., & Wei, L. (2010). Preparation, characterization and activity evaluation of heterostructure In2O3/In(OH)3 photocatalyst. *Journal of Hazardous Materials*, *180*(1), 735–740. https://doi.org/10.1016/j.jhazmat.2010.04.108

Tuzluca, F. N., Yesilbag, Y. O., & Ertugrul, M. (2018). Synthesis of In2O3 nanostructures with different morphologies as potential supercapacitor electrode materials. *Applied Surface Science*, *427*, 956–964. https://doi.org/10.1016/j.apsusc.2017.08.127

Vakh, C., & Koronkiewicz, S. (2023). Surfactants application in sample preparation techniques: Insights, trends, and perspectives. *TrAC Trends in Analytical Chemistry*, *165*, 117143. https://doi.org/10.1016/j.trac.2023.117143

Wiranwetchayan, O., Ruankham, P., Promnopas, W., Choopun, S., Singjai, P., Chaipanich, A., & Thongtem, S. (2018). Effect of nanoporous In2O3 film fabricated on TiO2-In2O3 photoanode for photovoltaic performance via a sparking method. *Journal of Solid State Electrochemistry*, *22*(8), 2531–2543. https://doi.org/10.1007/s10008-018-3968-1

Younis, A., & Osman, A. (2023). Solvent-free Organic Reaction Techniques as an Approach for Green Chemistry. *Journal of the Turkish Chemical Society Section A: Chemistry*, *10*(2), Article 2. https://doi.org/10.18596/jotcsa.1188983

Zatsepin, D. A., Boukhvalov, D. W., Zatsepin, A. F., Vines, L., Gogova, D., Shur, V. Ya., & Esin, A. A. (2019). Bulk In2O3 crystals grown by chemical vapour transport: A combination of XPS and DFT studies. *Journal of Materials Science: Materials in Electronics*, *30*(20), 18753–18758. https://doi.org/10.1007/s10854-019-02228-6

Zhu, L., Wang, Z., Wang, J., Liu, J., Zhang, J., & Yan, W. (2024). Pt-Embedded Metal–Organic Frameworks Deriving Pt/ZnO-In2O3 Electrospun Hollow Nanofibers for Enhanced Formaldehyde Gas Sensing. *Chemosensors*, *12*(6), Article 6. https://doi.org/10.3390/chemosensors12060093

Zhu, P., Wu, W., Zhou, J., & Zhang, W. (2007). Preparation of size-controlled In2O3 nanoparticles. *Applied Organometallic Chemistry*, *21*(10), 909–912. https://doi.org/10.1002/aoc.1300